

HOSTED BY



ELSEVIER

Contents lists available at ScienceDirect

Engineering Science and Technology, an International Journal

journal homepage: www.elsevier.com/locate/jestech

Full Length Article

An intelligent approach to optimize the EDM process parameters using utility concept and QPSO algorithm

Chinmaya P. Mohanty^a, Siba Sankar Mahapatra^{b,*}, Manas Ranjan Singh^c^a Faculty of Science and Technology, IFHE University, Hyderabad 501504, India^b National Institute of Technology, Rourkela 769008, India^c Silicon Institute of Technology, Bhubaneswar 751024, India

ARTICLE INFO

Article history:

Received 9 February 2016

Revised 28 June 2016

Accepted 6 July 2016

Available online xxxx

Keywords:

Electrical discharge machining

Utility concept

Quantum behaved particle swarm

optimization

Radial over cut

ABSTRACT

Although significant research has gone into the field of electrical discharge machining (EDM), analysis related to the machining efficiency of the process with different electrodes has not been adequately made. Copper and brass are frequently used as electrode materials but graphite can be used as a potential electrode material due to its high melting point temperature and good electrical conductivity. In view of this, the present work attempts to compare the machinability of copper, graphite and brass electrodes while machining Inconel 718 super alloy. Taguchi's L_{27} orthogonal array has been employed to collect data for the study and analyze effect of machining parameters on performance measures. The important performance measures selected for this study are material removal rate, tool wear rate, surface roughness and radial overcut. Machining parameters considered for analysis are open circuit voltage, discharge current, pulse-on-time, duty factor, flushing pressure and electrode material. From the experimental analysis, it is observed that electrode material, discharge current and pulse-on-time are the important parameters for all the performance measures. Utility concept has been implemented to transform a multiple performance characteristics into an equivalent performance characteristic. Non-linear regression analysis is carried out to develop a model relating process parameters and overall utility index. Finally, the quantum behaved particle swarm optimization (QPSO) and particle swarm optimization (PSO) algorithms have been used to compare the optimal level of cutting parameters. Results demonstrate the elegance of QPSO in terms of convergence and computational effort. The optimal parametric setting obtained through both the approaches is validated by conducting confirmation experiments.

© 2016 The Authors. Publishing services by Elsevier B.V. on behalf of Karabuk University. This is an open access article under the CC BY-NC-ND license (<http://creativecommons.org/licenses/by-nc-nd/4.0/>).

1. Introduction

Nickel based super alloys such as Inconel 718 and Inconel 713 are the class of metallic materials with excellent characteristic of toughness and resistance to high temperature, oxidation and corrosion. The high strength-to-weight ratio and corrosion resistance properties possessed by these alloys have led to a wide and diversified range of successful applications in aerospace and other industrial applications. Their capability to sustain mechanical strength at elevated temperature causes difficulty in machining with conventional machining processes. Due to these difficulties, it is difficult to machine Inconel 718 by conventional machining

processes using conventional tool materials. However, machining of composites, super alloys, and ceramics can be accomplished with ease by the use of non-conventional machining process like electrical discharge machining (EDM). In today's manufacturing scenario, EDM contributes a major share in manufacturing automobile parts, intricate part shapes, complex shaped dies and moulds and other industrial usages. In EDM process, the material removal takes place owing to a series of spark discharges through enormous amount of heat generation between the electrodes. The heat generated is enough to vaporize and melt material from both the electrodes. The molten material is flushed by dielectric fluid from the crater cavity in from of dirt and debris and the replica of the tool is transferred onto the work surface. However, accuracy and versatility of the process, economical machining and accurate prediction of performance measures are the major concerns for tool engineers and researchers till now.

Extensive literature review suggests that different studies on EDM focus on improvement/modification of the process to

* Corresponding author.

E-mail addresses: chinmaymohantymech@gmail.com (C.P. Mohanty), mahapatras2003@gmail.com (S.S. Mahapatra), manasranjan.singh@gmail.com (M.R. Singh).

Peer review under responsibility of Karabuk University.

<http://dx.doi.org/10.1016/j.jestech.2016.07.003>

2215-0986/© 2016 The Authors. Publishing services by Elsevier B.V. on behalf of Karabuk University.

This is an open access article under the CC BY-NC-ND license (<http://creativecommons.org/licenses/by-nc-nd/4.0/>).

enhance certain performance measures, control circuits, analysis on the microstructure of the machined surface and effect of machining parameters. Literature also reveals that only a few controllable machining parameters viz., pulse-on-time, discharge current and open circuit voltage mostly influence the performance measures of the EDM process [1–3]. In EDM copper and brass are frequently used electrode material. However, graphite can be used as a potential electrode material due to its high melting point temperature and good electrical conductivity. The temperature resistance property makes graphite a suitable electrode material. However, studies on analysis of machining efficiency of the process with variety of electrodes are extremely scarce in literature [4–5]. Moreover, the studies are limited to application of commonly used work-tool pairs, machines and shop conditions. Even though optimization of multiple machining characteristics is beneficial from practical point of view, little efforts have been made in this direction. Few studies report application of evolutionary algorithm like particle swarm optimization (PSO) to obtain the best process states of EDM process [6–8]. Due to the simple concept, easy implementation, and rapid convergence, PSO has gained much attention and been successfully applied to a wide range of applications such as job scheduling, power and voltage control, fiber-reinforced laminates problems [9–14]. Many studies report that QPSO with its global search ability can perform better than PSO [15–18]. However, past studies hardly provide any report to compare the effectiveness of both the algorithms in terms of obtaining the optimal level of machining parameters for multiple performance characteristics of EDM process.

In view of this, the present work focuses on experimental investigation on machinability of Inconel 718 super alloy in EDM process for the multiple performance characteristics viz. material removal rate (MRR), tool wear rate (TWR), surface roughness (SR), and radial overcut (RO) which are functions of process variables viz., open circuit voltage, discharge current, pulse-on-time, duty factor, flushing pressure and electrode material. The experimental architecture is planned as per Taguchi's L_{27} orthogonal array to extract maximum information from the study with limited number of experimental runs. Utility concept is used to convert the multiple performance measures into an equivalent single performance measure by calculating the overall utility index. Non-linear regression analysis is conducted to develop a valid empirical model relating process parameters and overall utility index. The model is further used as an objective function in quantum behaved particle swarm optimization (QPSO) and particle swarm optimization (PSO) algorithm to obtain optimal level of cutting parameters. The optimal solutions so obtained are compared to justify goodness of the algorithm in solving such a machining problem. Finally, the optimal levels of cutting parameters obtained in both the algorithms are validated through confirmation test. This model will help in selecting ideal process states during actual machining and increasing productivity of the process for tool engineers.

2. Literature review

In the past two decades, electrical discharge machining has emerged as a subject of extensive research among the non-conventional machining process. To improve the machining efficiency of the process various technological, statistical and numerical studies have been reported. Lee and Li [4] have experimentally analyzed the effect of process variables such as electrode material, polarity, discharge current, open circuit voltage, pulse duration, pulse interval and flushing pressure on material removal rate, relative wear ratio and surface roughness of tungsten carbide work piece. Prabhu and Vinayagam [19] have proposed a grey relational analysis and fuzzy logic approach for simultaneous optimization of

several performance characteristics of the process when dielectric fluid is mixed with carbon nano-tube (CNT). Dewangan and Biswas [20] have adopted Taguchi's experimental design combined with grey relational analysis for optimization of multiple responses such as material removal rate and tool wear rate of EDM using AISI P20 tool steel as the work piece material and copper as electrode.

Meena et al. [21] have analyzed the effect of various flushing conditions on the accuracy of deep holes drilled by micro-EDM. Beri et al. [22] have concluded that improved performance characteristics can be achieved with the use of copper-tungsten (CuW) electrode produced through powder metallurgy route in comparison with conventional copper electrode. Similarly, Senthilkumar and Reddy [23] have demonstrated that copper composite with 40% boron carbide reinforcement developed through powder metallurgy route exhibits better metal removal rate (MRR) and tool removal rate (TRR) compared to conventional copper electrode. Wang and Han [24] have proposed a three-dimensional model of flow field with liquid, gas and solid phases for the movement of debris and bubbles within the machining gap in EDM. The model is validated through experimentation with conclusion that bubble expansion becomes strong with the increase of the discharge current and pulse-on-time. Shen et al. [25] have investigated effect of different machining parameters such as inter electrode distance, pulse duration, polarity and electrode shape on energy distribution using titanium alloy as work piece. The results show that energy distribution characteristics are largely influenced by the power density applied on the electrodes.

Tripathy and Tripathy [26] have used Taguchi experimental design in combination with TOPSIS and Grey Relational Analysis (GRA) to optimize the process variables such as powder concentration, peak current, pulse on time, duty cycle and gap voltage on multiple responses such as MRR, TWR, EWR and SR. Talla et al. [27] have used aluminum powder in kerosene dielectric to improve the machining efficiency of the EDM process. The study showed an increase in MRR and improvement in surface quality of the machined surface compared to conventional EDM. Talla et al. [28] have studied the effect process parameters powder concentration, peak current, pulse on time and duty cycle on two performance measures viz. MRR and SR. The study revealed that the powder concentration of 6 g/L gives the best result to maximize MRR and minimize surface roughness. Many studies have recently reported that controlled cryogenic treatment of electrode and work piece materials improves the machining characteristics in EDM as well as wire-EDM for various work-tool combinations [29–32].

Numerical models have been proposed to study the process behavior to reduce the cost of experimentation and machining time. In this direction, Paramashivan et al. [33] have proposed a mathematical model which quantifies the aerosol generated from the die sinking EDM process while machining steel work piece with copper electrode. Joshi and Pande [34] have suggested a numeral model for EDM for prediction of performance characteristics such as material removal rate and tool wear rate using finite element method. The proposed model is also validated through experimentation by the same researchers [35]. Mohanty et al. [36] have proposed a non-dominated sorting genetic algorithm (NSGA-II) for multi-objective optimization of EDM parameters using a thermo-structural model. Chen and Mahdivian [37] have suggested a theoretical model to estimate the material removal rate and surface quality considering process parameters like discharge current and pulse duration. The theoretical results have shown to be in good agreement with experimental data.

In recent times, artificial intelligence (AI) techniques are extensively applied for process modelling and optimization of the process [38–41]. Padhee et al. [42] have used non-dominated sorted genetic algorithm (NSGA-II) to optimize MRR and surface roughness for machining parameters such as concentration of silicon

powder in the dielectric fluid, pulse-on-time, duty cycle and peak current. Pradhan and Biswas [43] have proposed neuro-fuzzy and neural network models for prediction of material removal rate, tool wear rate and radial overcut when AISI D2 steel is machined with copper electrode. Pradhan and Das [44] have proposed an Elman network for the prediction of material removal rate for EDM process. Yang et al. [45] have employed simulated annealing in conjunction with artificial neural network for optimization of materials removal rate and surface roughness.

Critical review of past studies suggests that a good amount of work is devoted towards technological enhancement and statistical and numerical modelling to improve and analyse EDM process. However, reports to analyse the machining efficiency of the process with different electrode materials seems to be less. Furthermore, it is also observed that limited number of attempts have been made to machine a relatively low conductive material like Inconel 718 which has a diversified application in aerospace engineering. Inconel 718, an aerospace material has abundant usage in manufacturing of components for liquid fueled rockets, rings and casings, sheet metal parts for aircraft, land-based gas turbine engines, cryogenic tank fasteners and instrumentation parts. Literature review reveals that few studies have been reported to obtain the optimal parametric setting for EDM process applying PSO algorithm [6-8]. Numerous studies reported that QPSO with the global search ability can achieve better results than PSO [15-18]. However, it is also observed that no attempt has been reported in application of utility concept in combination with QPSO to obtain the best parametric setting for EDM. Therefore, there exist a vital need to compare and check the effectiveness of both the algorithms to find the optimal level of machining parameters.

3. Utility concept

According to Walia et al. [46] the overall usefulness of a process can be denoted by a unified index called as utility which is the sum of the individual utilities of various quality characteristics of the process. If V_r is the measure of effectiveness of an attribute (or quality characteristic) r and there are n attributes estimating the outcome space, then the joint utility function can be expressed as [46-47].

$$U(V_1, V_2, \dots, V_n) = f(U_1(V_1), U_1(V_1), \dots, U_n(V_n)) \quad (1)$$

where $U_r(V_r)$ is the utility of the r th attribute.

If the attributes are independent, the overall utility function is the sum of individual utilities and can be calculated as

$$U(V_1, V_2, \dots, V_n) = \sum_{r=1}^n U_r(V_r) \quad (2)$$

After assigning weights to the attributes, the overall utility function can be calculated as

$$U(V_1, V_2, \dots, V_n) = \sum_{r=1}^n W_r U_r(V_r) \quad (3)$$

where W_r is the weight assigned to the attribute r .

In this work, there are four attributes and equal weight i.e. 0.25 has been assigned to each attributes. The utility value for each quality characteristic is estimated by a preference scale. The acceptable and the best value of the quality characteristic are assigned two arbitrary numerical values 0 and 9 (preference number) respectively and the preference number P_r can be expressed on a logarithmic scale as

$$P_r = A \times \log \frac{X_r}{X_r^*} \quad (4)$$

where X_r represents quality characteristic of any value and X_r^* represents just an acceptable value of quality the characteristic r and A has been used as a constant. Here, value of A can be calculated by equation 5 and if $X_r = X_r^*$, then preference number will be 9 where X_r^* is the optimal or best value.

$$A = \frac{9}{\log \frac{X_r}{X_r^*}} \quad (5)$$

The overall utility index can be calculated as

$$U = \sum_{r=1}^n W_r P_r \quad (6)$$

$$\text{Subject to condition that } \sum_{r=1}^n W_r = 1 \quad (7)$$

In this work, overall utility index serves as the single performance measure objective value for optimization which has been accumulated from utility values of individual performance characteristic.

4. Particle swarm optimization

Particle swarm optimization (PSO) algorithm, originally introduced by Kennedy and Eberhart [9], is a population based evolutionary computation method influenced by the behavior of organisms such as bird flocking and fish schooling. In PSO, each member is called particle and each particle moves around in the search space with a velocity which is continuously updated by the particle's individual contribution and the contribution of the particle's neighbors or the contribution of the whole swarm. The members of the whole population are maintained during the search procedure so that information can be socially shared among all individuals to direct the search towards the best position in the search space. Each particle moves towards its best previous position and towards the best particle in the whole swarm called the g_{best} based on the global neighborhood. Each particle moves towards its best previous position and towards the best particle in its restricted neighbourhood based on the local variant so called the p_{best} model. PSO is basically characterized as a simple heuristic of well-balanced mechanism with flexibility to progress and adjust to both global and local exploration capabilities. All the particles tend to converge to the best solution rapidly even in the local version in most cases as compared to genetic algorithm. Due to the simple concept, easy implementation, and rapid convergence, PSO has gained much attention and been successfully applied to a wide range of applications viz. as job scheduling, power and voltage control problems [11-12].

In PSO, the initial population is generated randomly and parameters are initialized. After evaluation of the fitness function, the PSO algorithm repeats the following steps iteratively:

- Personal best (best value of each individual so far) is updated if a better value is discovered.
- Then, the velocities of all the particles are updated based on the experiences of personal best and the global best in order to update the position of each particle with the velocities currently updated.

After finding the personal best and global best values, velocities and positions of each particle are updated using Eqs. (8) and (9) respectively.

$$v_{ij}^t = w^{t-1} v_{ij}^{t-1} + c_1 r_1 (p_{ij}^{t-1} - x_{ij}^{t-1}) + c_2 r_2 (g_{ij}^{t-1} - x_{ij}^{t-1}) \quad (8)$$

$$x_{ij}^t = x_{ij}^{t-1} + v_{ij}^t \quad (9)$$

where v_{ij}^t represents velocity of particle i at iteration t with respect to j th dimension ($j = 1, 2, \dots, n$). p_{ij}^t represents the position value of the i th personal best with respect to the j th dimension g_{ij}^t represents the global best (g_{best}) i.e. the best of p_{best} among all the particles. x_{ij}^t is the position value of the i th particle with respect to j th dimension. c_1 and c_2 are positive acceleration parameters which provide the correct balance between exploration and exploitation and are called the cognitive parameter and the social parameter respectively. r_1 and r_2 are the random numbers provide a stochastic characteristic for the particles velocities in order to simulate the real behavior of the birds in a flock. The inertia weight parameter w is a control parameter which is used to control the impact of the previous velocities on the current velocity of each particle. Hence, the parameter w regulates the trade-off between global and local exploration ability of the swarm. The recommended value of the inertia weight w is to set it to a large value for the initial stages in order to enhance the global search of the search space and gradually decrease it to get more refined solutions facilitating the local search in the last stages. In general, the inertia weight is set according to the following Eq. (10) [48].

$$w = w_{max} - \frac{w_{max} - w_{min}}{iter_{max}} \times iter \quad (10)$$

where w_{min} and w_{max} are initial and final weights and $iter_{max}$ is the maximum number of iterations and $iter$ is the current iteration number.

4.1. Quantum behaved particle swarm optimization (QPSO)

The main drawback of the PSO algorithm is that it does not assure global convergence because it is trapped into local optima although it converges fast and loose its exploration-exploitation ability. The reason being that the velocity vectors assume very small values as iterations proceed. Clerc and Kennedy [49] have presented that PSO is capable to find a reasonable quality solution much faster than other evolutionary algorithms but it cannot improve the quality of the solution as the number of generations is increased. If p_{best} and g_{best} of a particle stay very close to each other then it becomes inactive in the swarm. In other words, when $(p_{ij}^{t-1} - x_{ij}^{t-1})$ and $(g_{ij}^{t-1} - x_{ij}^{t-1})$ are both small in Eq. (8) and at the same time v_{ij}^t has a small value then this particle loses its exploration ability. This could happen at early stages for the g_{best} particle and as a consequence the PSO is trapped in local minima. QPSO is proposed and stimulated to avoid the drawbacks of original PSO. In the quantum PSO, the state of a particle is described by wave function $\Psi(x, t)$ instead of velocity. The difference between QPSO and classical PSO is the dynamic behavior of the particle i.e. the exact values of x and v cannot be determined simultaneously in QPSO. The probability of the particle's appearing in position x can be learnt from probability density function $|\Psi(x, t)|^2$. The probability density function is used to estimate the probability distribution function of the particle's position.

Employing the Monte-Carlo method, the particle position is updated according to the following equations,

$$X_{i,(t+1)}^j = P_{i,(t+1)}^j - \beta * (M_{Best_t^j} - X_{i,t}^j) * \ln(1/u) \text{ if } k \geq 0.5 \quad (11)$$

$$X_{i,(t+1)}^j = P_{i,(t+1)}^j + \beta * (M_{Best_t^j} - X_{i,t}^j) * \ln(1/u) \text{ if } k < 0.5 \quad (12)$$

$$P_{i,(t+1)}^j = \theta * P_{Best_{i,t}^j} + (1 - \theta) * g_{Best_t^j} \quad (13)$$

$$M_{Best_t^j} = \frac{1}{N} \sum_{i=1}^N P_{Best_{i,t}^j} \quad (14)$$

where P_i is the local attractor, $P_{Best_{i,t}^j}$ is the best positions which the of particle i at iteration t with respect to j th dimension has achieved so far and $g_{Best_t^j}$ is the best position of all particles in current generation. $M_{best_t^j}$ is the mean best position which is defined as the mean of all the best positions of the population in current generation, $k, u, \theta, k, u, \theta$ are random numbers distributed uniformly on $[0, 1]$. β in Eqs. (11) and (12) is the tuning parameter to control the convergence speed of the particle and is called as contraction expansion (CE) coefficient. Value of β is tuned from 1 to 0.4 for initially accommodating a more global search with an objective to terminate the QPSO algorithm with a better local search.

The β value is adaptively allocated as per the Eq. (15)

$$\beta = \beta_{max} - \{(\beta_{max} - \beta_{min}) / iteration_{max}\} * iter \quad (15)$$

where β_{max} is the initial contraction expansion factor value, β_{min} is the final contraction expansion factor value, $iter$ is the current iteration number and $iteration_{max}$ is the maximum number of iterations. The termination criterion for the algorithm is the maximum number of iterations. The pseudo code for the search procedure of the QPSO given below. Fig. 1 shows the flow chart of the QPSO algorithm.

The pseudo code of proposed QPSO

Initialize the population size, the current position and the dimensions of the particles;

While (termination condition i.e. maximum Iteration)

Do

$t=t+1$;

Compute the mean best position M_{Best} by Eq. (14);

Select a value of β by Eq. (15);

for $i=1$ to population size

for $j=1$ to dimensions of the particles

If $k \geq 0.5$

else

$$X_{i,(t+1)}^j = P_{i,(t+1)}^j + \beta * (M_{Best_t^j} - X_{i,t}^j) * \ln(1/u);$$

end if

end for

Evaluate the fitness value of $X_{i,(t+1)}$, that is the objective function

Update the $p_{Best_{i,t}^j}$ and $g_{Best_{i,t}^j}$

end for

end do

end

5. Experimental details

In this work, Taguchi method, a powerful tool for parametric analysis of the performance characteristics is used to extract maximum information with least number of experimental runs. Computer numerical control (CNC) die sinking EDM machine (ECOWIN PS 50ZNC) with servo-head (constant gap) is used for conducting the experiment. Paraffin oil of specific gravity of 0.820 is used as dielectric fluid with positive polarity for electrode with side flushing to conduct the experiments. Inconel alloy 718, a nickel-chromium alloy characterized by high-strength, high corrosion-resistant, good tensile and high creep rupture strength has been used as the work material in this study. The chemical composition of the materials is given in Table 1. Table 2 shows the thermal property of the work material. The X-ray diffraction plot of the Inconel 718 sample used in the present study is shown in Fig. 2. It clearly shows that there are no peaks other than γ -phase (austenite) phase which corresponds to face-centred cubic

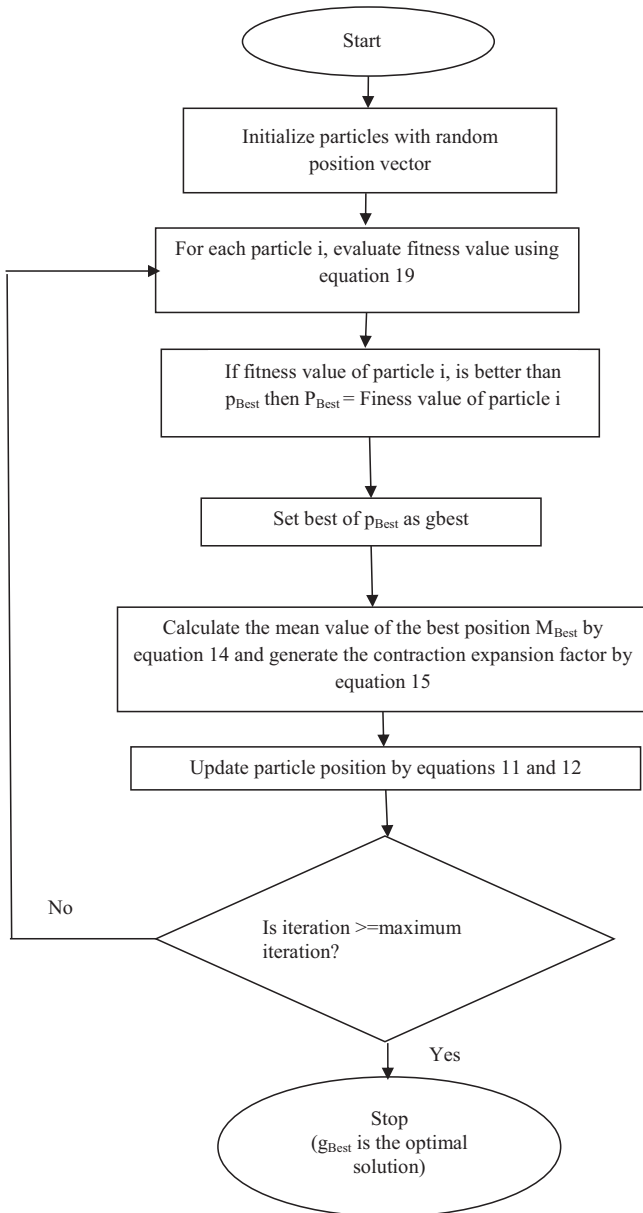


Fig. 1. Flow chart of QPSO algorithm.

Ni-based γ -phase of Inconel 718 super alloy. The sharp peak of the diffraction patterns reveals the crystalline nature of the alloy.

In EDM process, the tool has to deal with a series of spark discharges. Hence, the tool must be of a good conductive material with high melting temperature, ability to withstand against high temperature and dissipate the heat. Therefore, commercially available brass, copper, and graphite are used as the electrode material. The machining diameters of the three electrodes are in cylindrical shape of diameter 13.5 mm. The EDM process is accomplished on Inconel 718 alloy plate of 8 mm thickness and $10 \times 11.5 \text{ cm}^2$ cross sectional area. Each experiment runs for 30 min. For weighing pur-

pose, the work piece and the electrodes are detached from the machine after each observation and cleaned and dried out. A precision electronic balance (accuracy 0.01 g) is used for measuring the weights of the work and tool materials before and after machining. Surface roughness tester (Surftest SJ 210, Mitutoyo) is used for measuring the surface quality. A tool maker's microscope (Carl Zeiss) is used for measuring the crater diameter on the machined surface on the work material.

The weight loss due to machining of work material noted before and after machining is used to calculate the material removal rate (MRR) using Eq. (16).

$$\text{MRR} = \frac{1000 \times \Delta W_w}{\rho_w \times T} \quad (16)$$

where ΔW_w is difference in weight of work material during machining, ρ_w is the density of work material and T is the machining time.

The weight loss due to machining of tool material noted before and after machining is used to calculate tool wear rate (TWR) using Eq. (17).

$$\text{TWR} = \frac{1000 \times \Delta W_t}{\rho_t \times T} \quad (17)$$

where ΔW_t is difference in weight of tool material during machining and ρ_t is the density of tool material ($\rho_{\text{brass}}=8565 \text{ kg/m}^3$, $\rho_{\text{copper}}=8960 \text{ kg/m}^3$ and $\rho_{\text{graphite}}=2130 \text{ kg/m}^3$).

Mitutoyo (Surftest SJ 210) is used to complete the surface roughness (SR) measurements on the machined surface of the work material. Five readings on the traverse direction of the machined surface are taken and average of five readings of surface roughness values are noted down.

The high temperature gradient developed due to series spark of discharges causes dimensional irregularities on the machined edges of the crater cavity. The deviation between the maximum diameter of the cavity and electrode diameter is called radial overcut. Although sufficient compensations are being provided during design of the tool and machining, radial overcut is quite common in EDM process. Minimization of overcut is essential for precise and accurate EDMed machining. Radial overcut is given by relation

$$\text{RO} = \frac{d_w - d_t}{2} \quad (18)$$

Here, d_w is the maximum diameter of the crater cavity and d_t is the diameter of the tool.

Fig. 3 shows the work material Inconel 718 after machining with three electrodes. Table 3 shows process parameters and their levels. Table 4 shows the L_{27} orthogonal array along with obtained responses and overall utility index.

6. Result and discussion

Taguchi's L_{27} orthogonal array (experimental design) along with obtained performance measures and the overall utility index have been depicted in Table 4. Analysis of variance (ANOVA) is carried out on performance measures such as material removal rate, tool wear rate, surface roughness and radial over cut with a view to analyse the effect of important process parameters. Table 5 shows the ANOVA table for MRR. For MRR, tool material is found to be the

Table 1
Chemical composition of Inconel 718 sample used in the study.

Chemical	C%	Si%	Mn%	S%	P%	Cr%	Fe%	Mo%	Co%	Nb%	Cu%	V%	Al%	Ti%	W%	Ni%
Amount	0.039	0.027	0.032	0.005	0.008	17.21	20.143	3.121	0.086	4.989	0.009	0.015	0.568	0.816	0.214	52.739

Table 2
Thermal properties of Inconel 718.

Properties	Density	Melting Temperature	Thermal Conductivity	Thermal expansion	Poissons ratio
Value	8190 kg/m ³	1609 K	15 W/m.K	13.0 μm/m°C	0.27–0.3

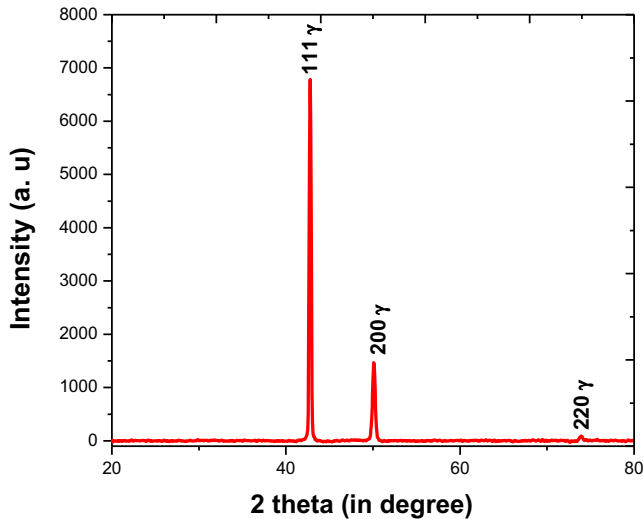


Fig. 2. X-ray diffraction plot of the Inconel 718 work material.

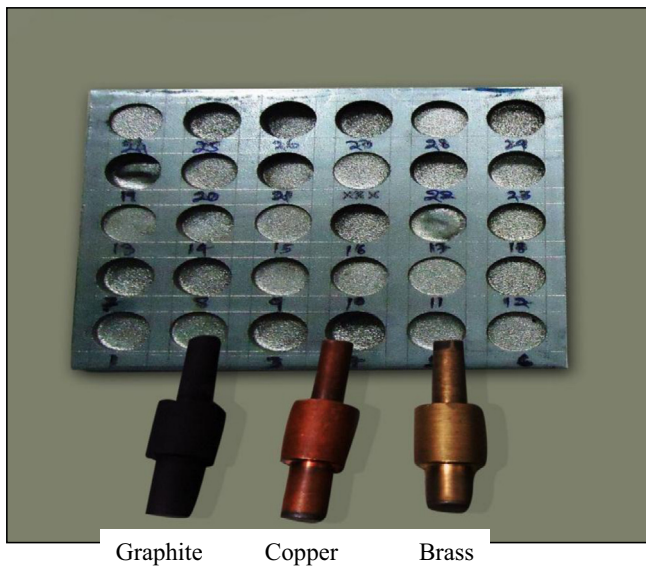


Fig. 3. Work material Inconel 718 after machining with three electrodes.

Table 3
Process parameters and their levels.

Process Parameters	Units	Levels		
		1	2	3
Open circuit voltage (A)	Voltage	70	80	90
Discharge current (B)	Ampere	3	5	7
Pulse-on-time (C)	Microsecond	100	200	300
Duty factor (D)	Percentage	80	85	90
Flushing pressure (E)	Bar	0.2	0.3	0.4
Tool material (F)		Brass	Copper	Graphite

most important process parameter with a percentage contribution of 58.04% followed by discharge current, pulse-on-time, duty factor, open circuit voltage and interactions terms discharge current × tool and pulse-on-time × tool with percentage contributions of 22.7%, 12.33%, 2.63%, 2.27%, 0.90% and 0.79% respectively. Flushing pressure is found to be an insignificant parameter for MRR with a percentage contribution of 0.12%. Table 6 shows the ANOVA for TWR. The table shows that tool material is again found to be the most important process parameter with a percentage contribution of 84.04%, followed by discharge current, pulse-on-time, and interactions terms like discharge current × tool with percentage contributions of 7.71%, 6.29% and 0.51% respectively. Flushing pressure, duty factor and open circuit voltage are found to be an insignificant parameter for TWR with a percentage contribution of 0.3%, 0.14% and 0.05% respectively. Table 7 shows the ANOVA table for overall utility index and it indicates that discharge current is the most influential parameter with a percentage contribution of 51.20% followed by tool material, pulse-on-time, open circuit voltage and interaction terms such as discharge current × tool and pulse-on-time × tool with percentage contribution of 18.98%, 15.09%, 4.82%, 2.31%, and 1.66% respectively. Flushing pressure and duty factor are found to be insignificant parameters with percentage contribution of 1.08%, and 0.77% respectively. Similarly, analysis of variance for surface roughness reveals that tool material is the most influential process parameter with percentage contribution of 72.71% followed by discharge current, pulse-on-time, interaction terms like discharge current × tool with percentage contribution of 36.38%, 3.16% and 0.42% respectively. Parameters such as open circuit voltage, duty factor and flushing pressure have little effect on surface roughness with a percentage of contribution of 0.26%, 0.08% and 0.04% respectively. Analysis of variance for radial overcut reveals that tool material, discharge current, pulse-on-time and interaction term discharge current × tool are the important process parameters with percentage contribution of 83.09%, 10.36%, 2.21% and 1.03% respectively. Open circuit voltage, duty factor and flushing pressure have little effect on radial overcut with a percentage contribution of 0.45%, 0.39% and 0.16% respectively. A scanning electron microscope (SEM) micrograph analysis is also carried out to study the formation of recast layers on the machined surface after machining. From the SEM micrographs, it is observed that recast layer thickness increases with increase in spark energy while machining with graphite and copper electrode. However, brass electrode at smaller spark discharges produces thinner recast layer in comparisons with graphite and copper electrodes.

Fig. 4 shows the main effect plot for MRR. The plot shows that the MRR decreases with increase of open circuit voltage from 70 V to 90 V but the decreases is more pronounced between 70 V and 80 V. Low values of open circuit voltage can lead to higher MRR whereas higher values of open circuit voltage can cause relatively lower material removal rates. However, the effect of open circuit voltage on MRR is not significant in comparison with discharge current. The figure indicates that material removal rate increases rapidly with the increase of discharge current from 3A to 7A. Increase in discharge current directly increases the spark energy which in turn causes an increase in the crater dimension resulting in higher removal of metal from the work surface. The figure shows that material removal rate decreases with increase in pulse-on-time and the decrease is rapid when pulse-on time is set beyond 200 μs. Increasing the pulse-on-time means applying

Table 4 L_{27} orthogonal array along with responses.

Run order	A	B	C	D	E	F	MRR in mm ³ /min	TWR in mm ³ /min	SR in μm	RO in mm	Overall utility index
1	70	3	100	80	0.2	Brass	11.5221	6.8540	8.4179	0.0282	5.8440
2	70	3	100	80	0.3	Copper	25.5444	4.5742	14.2626	0.1076	5.2514
3	70	3	100	80	0.4	Graphite	31.7515	3.5681	19.3699	0.2563	4.5499
4	70	5	200	85	0.2	Brass	12.1862	7.2991	11.1324	0.0780	4.5216
5	70	5	200	85	0.3	Copper	27.5620	4.8501	19.0233	0.2557	4.0588
6	70	5	200	85	0.4	Graphite	38.3034	3.2952	25.0787	0.4354	3.6527
7	70	7	300	90	0.2	Brass	22.5026	7.1806	18.3226	0.1818	3.5755
8	70	7	300	90	0.3	Copper	33.4826	5.2938	24.0778	0.2838	3.6078
9	70	7	300	90	0.4	Graphite	40.8613	3.0006	30.2353	0.4450	3.5734
10	80	3	200	90	0.2	Copper	23.9502	4.2463	14.0796	0.1464	5.0969
11	80	3	200	90	0.3	Graphite	32.5885	2.6482	20.3344	0.3364	4.4646
12	80	3	200	90	0.4	Brass	6.3664	7.0477	7.7977	0.0734	4.6651
13	80	5	300	80	0.2	Copper	14.8303	3.8907	20.4310	0.3056	3.6324
14	80	5	300	80	0.3	Graphite	26.2129	2.4188	25.6183	0.4877	3.0508
15	80	5	300	80	0.4	Brass	3.3944	6.9065	12.4431	0.0708	3.4151
16	80	7	100	85	0.2	Copper	37.7847	6.1202	21.0403	0.2659	3.7487
17	80	7	100	85	0.3	Graphite	47.6497	3.9141	27.4052	0.4790	3.4744
18	80	7	100	85	0.4	Brass	21.6813	8.9148	13.9793	0.1232	3.9462
19	90	3	300	85	0.2	Graphite	16.4502	2.2543	22.3897	0.3899	3.7696
20	90	3	300	85	0.3	Brass	4.4495	6.3105	9.1573	0.0315	4.9417
21	90	3	300	85	0.4	Copper	12.3846	3.4282	17.2583	0.2355	4.1719
22	90	5	100	90	0.2	Graphite	39.7088	3.7379	24.9953	0.4058	3.4782
23	90	5	100	90	0.3	Brass	15.2592	8.4282	9.5444	0.0736	4.7791
24	90	5	100	90	0.4	Copper	31.3547	5.5108	18.4393	0.2132	4.1549
25	90	7	200	80	0.2	Graphite	41.3635	3.7707	26.5567	0.4544	3.4088
26	90	7	200	80	0.3	Brass	14.4506	7.9370	15.0112	0.0929	3.8953
27	90	7	200	80	0.4	Copper	30.1753	5.4724	21.7047	0.2877	3.6264

Table 5

ANOVA for MRR.

Source	DF	Seq SS	Adj SS	Adj MS	F	P	% Contribution
Open circuit voltage	2.0000	92.5100	92.5100	46.2600	30.5400	0.0010	2.270708
Discharge current	2.0000	927.7300	927.7300	463.8700	306.2500	0.0000	22.77163
Pulse-on-time	2.0000	498.4200	498.4200	249.2100	164.5300	0.0000	12.23399
Duty factor	2.0000	107.1900	107.1900	53.6000	35.3800	0.0000	2.631036
Flushing pressure	2.0000	5.1300	5.1300	2.5600	1.6900	0.2610	0.125919
Tool	2.0000	2364.5900	2364.5900	1182.3000	780.5700	0.0000	58.04014
Discharge current \times Tool	4.0000	36.8300	36.8300	9.2100	6.0800	0.0260	0.904012
Pulse-on-time \times Tool	4.0000	32.5700	32.5700	8.1400	5.3800	0.0350	0.799448
Residual error	6.0000	9.0900	9.0900	1.5100			
Total	26.0000	4074.0600					

Table 6

ANOVA for TWR.

Source	DF	Seq SS	Adj SS	Adj MS	F	P	% Contribution
Open circuit voltage	2.0000	0.0523	0.0523	0.0261	0.2900	0.7570	0.053926
Discharge current	2.0000	7.4812	7.4812	3.7406	40.9700	0.0000	7.713858
Pulse-on-time	2.0000	6.1046	6.1046	3.0523	33.4300	0.0000	6.294447
Duty factor	2.0000	0.1359	0.1359	0.0679	0.7400	0.5000	0.140126
Flushing pressure	2.0000	0.2933	0.2933	0.1466	1.6100	0.2480	0.302421
Tool	2.0000	81.5084	81.5084	40.7542	446.3800	0.0000	84.04323
Discharge current \times Tool	4.0000	0.4953	0.4953	0.1238	1.3600	0.3160	0.510703
Residual error	10.0000	0.9130	0.9130	0.09130			
Total	26.0000	96.9839					

the same heat flux for longer duration. The pressure inside the plasma channel decreases due to continuous application of the same heat flux for longer duration. Since the volume of molten metal remains unaffected, further increase in pulse-on-time results in decrease of MRR. MRR increases monotonically with increase of duty factor. Increase in duty factor causes an increase in the spark energy across the gap between the electrodes resulting in increase of temperature which ultimately leads to increase in MRR. Similar observations have been reported in experimental observation of Pradhan and Biswas [43]. Material removal is higher while machining with graphite electrode followed by copper and brass respec-

tively. Copper and graphite electrodes have higher thermal conductivity and higher melting point temperature whereas brass electrode having smaller thermal conductivity and lower melting point temperature. Subsequently, the spark energy across graphite and copper electrodes are higher which in turn removes higher material than brass electrode.

The machining cost of the EDM process is largely affected by erosion rate of tool. Fig. 5 shows the main effect plot of TWR with important process parameters. The plot shows that tool erodes rapidly with increase in discharge current. Increase in discharge current increases the spark energy and hence more heat is

Table 7
ANOVA for overall utility index.

Source	DF	Seq SS	Adj SS	Adj MS	F	P	% contribution
Open circuit voltage	2.0000	2.3922	2.3922	1.1961	3.5900	0.0940	4.829654
Discharge current	2.0000	25.3644	25.3644	12.6822	38.0800	0.0000	51.20862
Pulse-on-time	2.0000	7.4792	7.4792	3.7396	11.2300	0.0090	15.09989
Duty factor	2.0000	0.3838	0.3838	0.1919	0.5800	0.5900	0.77486
Flushing pressure	2.0000	0.5398	0.5398	0.2699	0.8100	0.4880	1.089812
Tool	2.0000	9.4018	9.4018	4.7009	14.1200	0.0050	18.98146
Discharge current \times Tool	4.0000	1.1486	1.1486	0.2871	0.8600	0.5360	2.318928
Pulse-on-time \times Tool	4.0000	0.8235	0.8235	0.2059	0.6200	0.6660	1.662578
Residual error	6.0000	1.9982	1.9982	0.3330			
Total	26.0000	49.5315					

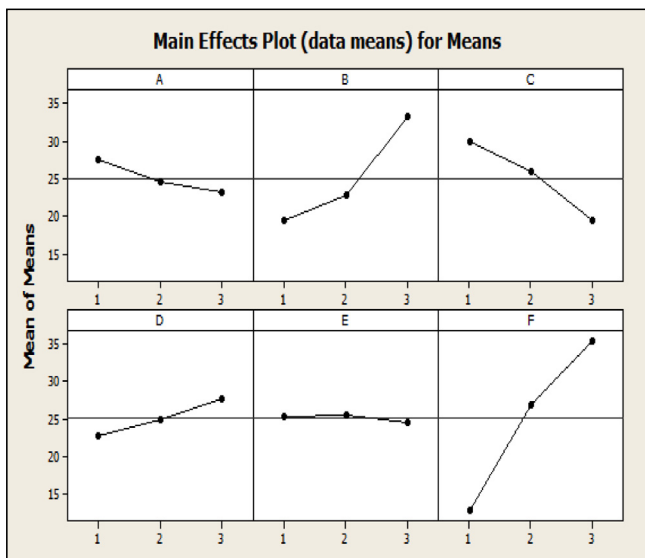


Fig. 4. Main effect plot of MRR.

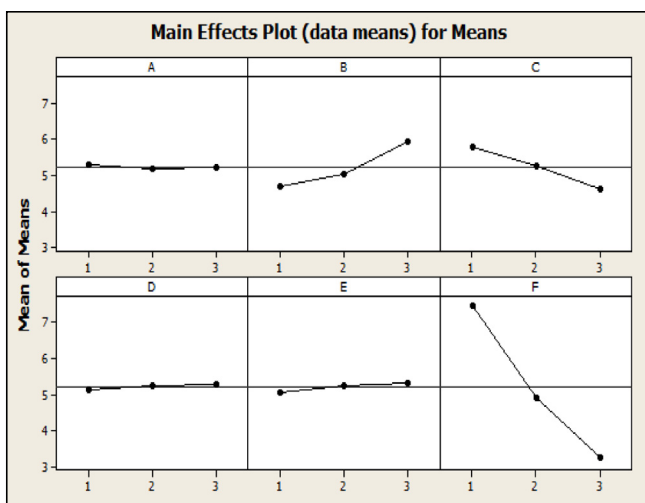


Fig. 5. Main effect plot of TWR.

generated across the electrodes resulting in higher melting and evaporation of the electrodes. The plot also shows that tool wear rate varies inversely with pulse-on-time. As conductivity of tool materials is higher than that of work material, the discharge of heat at the time of machining from the tool material is quick in comparison to work material. Therefore, tool wear decreases at higher pulse-on-time. Attachment of carbon particles onto the sur-

face of tool is another reason of low tool wear rate at high pulse-on-time. While machining Inconel 718, erosion of tool is faster with the use of brass tool followed by copper and graphite tool. Erosion of tool with graphite electrode is minimum due to its extremely high melting point temperature. As graphite and copper have reasonably high melting point temperature and good thermal conductivity than brass tool, the erosion rate of brass tool is faster in comparison to other electrodes. The figure also shows that open circuit voltage, duty factor and flushing pressure do not contribute much for the variation of TWR.

The machined surface quality and crater dimension mainly depends up the discharge energy. Higher the discharge energy, higher is the material removed which in turn produces poor surface quality. Fig. 6 shows the main effect plot of surface roughness through which analysis of the effect of various machining parameters on surface quality has been made. It shows that surface quality deteriorates with increases in discharge current. The discharge energy is directly governed by discharge current. Hence, more heat is produced between the electrodes resulting in larger size material to be removed from the work surface. This degrades the surface quality produced on the machined surface. The plot also indicates surface roughness increases with increase in pulse-on-time gradually. Increase in pulse-on-time increases the spark energy across electrodes which in turn cause larger size material to be removed from work surface degrading the surface quality. Inconel 718 work material machined with graphite electrode produces the poorest performance with regard to the surface finish. Brass electrode at smaller values of discharge energy produces an excellent surface quality while machining Inconel 718. The work material while

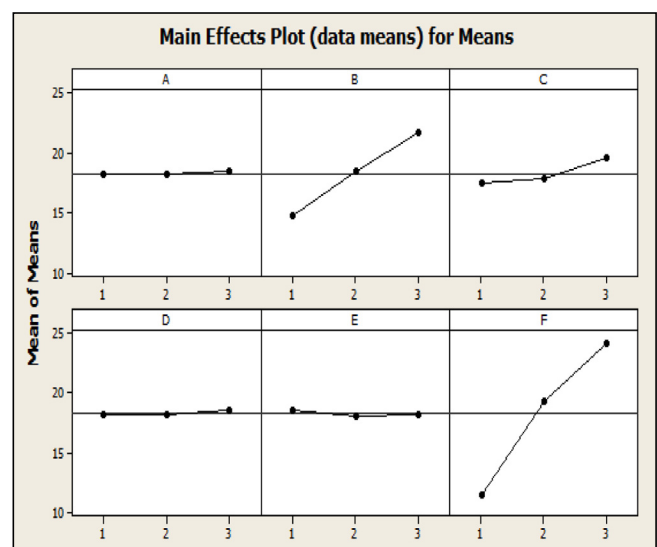


Fig. 6. Main effect plot of Surface roughness.

machining with copper electrode produces surface quality between those of brass and graphite. The size of material removed by graphite and copper electrodes is larger on the machined surface. It decreases the surface quality produced whereas brass electrode at the smaller value of discharge energy produces finest surface quality at the expense of more tool erosion. Hence, it can be concluded that good surface quality can only be produced at smaller value of spark energy with brass as the electrode material. The effect of open circuit voltage, duty factor and flushing pressure for variation of surface roughness is minimal. Yet, it is observed that surface roughness increases slowly with increase in open circuit voltage.

In EDM, precise and accurate machining means reduction of overcut. Fig. 7 shows the variation of radial overcut with important process parameters. It shows that radial overcut varies directly with increase in discharge current. Higher values discharge current causes increase in spark energy resulting in increase of temperature between the tool and work material and thus producing wider and larger craters on the machined surface. This, in turn, increases the radial overcut. The plot also shows that radial overcut increases gradually with increase of pulse-on-time. Increase of pulse-on-time causes prolonged occurrence of sparks on the machined surface. It results in increase of the radial overcut on the machined surface due to increase in spark energy. However, it observed that the effect of discharge current on radial overcut is higher as compared to pulse-on-time. Radial overcut is higher while machining with graphite electrode followed by copper and brass electrode respectively. As craters produced in graphite and copper electrodes are wider and larger, radial overcut on the machined surface is also larger. Thus, it can be concluded that brass electrode at the smaller value of spark energy can be used for producing precise and accurate EDMed parts at the expense of more tool erosion. The other factors such as open circuit voltage, duty factor and flushing pressure hardly contribute to radial overcut in comparison to discharge current, pulse-on-time and tool material.

In this work, utility concept has been used to convert the multiple performance measures into an equivalent single performance measure by calculating the overall utility index. The single performance measure is ranked between 0 to 9 with highest value of overall utility index of 5.84. The process model relating overall utility index with process parameters have been developed through non-linear regression analysis using SYSTAT software has been shown in Eq. (19). The coefficient of determination (R^2) and

adjusted R^2 values are found to be 98.9% and 99.1% respectively which confirms the validation of the model.

$$\begin{aligned} \text{Overall utility index}(U) = & -0.010 + 0.709 \times A - 0.310 \times B \\ & - 0.015 \times C - 0.477 \times D + 8.499 \times E \\ & - 1.637 \times F + 0.002 \times A^2 - 0.011 \times B^2 \\ & + 0.009 \times D^2 - 15.592 \times E^2 + 0.114 \times F^2 \\ & + 0.073 \times B \times F + 0.004 \times C \times F \\ & - 0.001 \times B \times C - 0.012 \times A \times D \quad (19) \end{aligned}$$

Present work aims at maximizing MRR and minimizing TWR, surface roughness and over cut which are functions of process parameters viz. open circuit voltage, discharge current, pulse-on-time, duty factor, flushing pressure and tool material. In this work, PSO and QPSO algorithm have been proposed to obtain the optimal parametric setting with an objective to maximize MRR and minimize TWR, surface roughness and radial over cut. The QPSO and PSO algorithms are coded in MATLAB 14 and run on a Pentium IV desktop. The empirical relation between process parameters and overall utility index obtained through non-linear regression analysis is used as objective function (Eq. (19)) for solving the optimization problem. Open circuit voltage, discharge current, pulse-on-time, duty factor, flushing pressure are quantitative process parameters whereas tool material is a qualitative process parameter. The quantitative parameters are real values that lie within the scope of experiment set up as shown in Table 1. The qualitative parameters are coded in the algorithm as 1 as brass tool, 2 as copper tool and 3 as graphite tool. For the qualitative parameter tool material, the nearest integer part of the real numbers has been considered. The range of qualitative parameter (tool material) are considered in the manner if the values lie in the range [1–1.4], it is treated as 1 or brass tool, [1.7–2.3] as 2 or copper tool and [2.4–3] as 3 or graphite tool. Fig. 8 shows the convergence of QPSO and PSO algorithms. The figure illustrates the performance of both the algorithms. It is convincible to note that QPSO algorithm is superior to PSO as it converges rapidly towards the best solution. It can be observed that after end of 100 iterations, the value of overall utility index is obtained as 6.91 for QPSO whereas the value for PSO is 6.52. The overall utility index value obtained through QPSO algorithm is higher than the overall utility index shown in Table 3 and PSO algorithm. Once the optimal parametric settings have been identified, it is mandatory to validate the same through

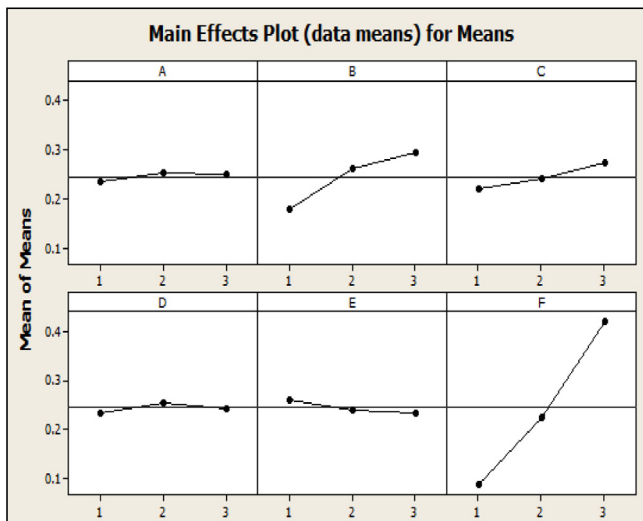


Fig. 7. Main effect plot of radial over cut.

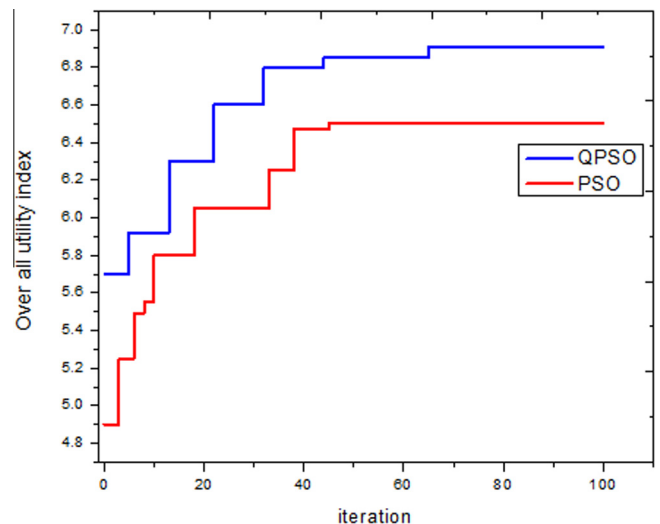


Fig. 8. Convergence curve for QPSO and PSO algorithm.

Table 8
Confirmative test result for optimal parametric setting.

Algorithm	Optimal parametric setting						MRR mm ³ /min	TWR mm ³ /min	Surface roughness μm	Radial overcut mm	Overall utility index from algorithm	Overall utility index from confirmatory test	Error %
	Voltage	Discharge current	Pulse- on-time	Duty factor	Flushing pressure	Tool							
QPSO	80 V	6 A	100 μs	80%	0.2 bar	Brass	26.5600	6.3100	7.2100	0.0732	6.9100	6.2100	10.1
PSO	75 V	5 A	180 μs	85%	0.2 bar	Brass	25.0100	6.5900	7.7500	0.0874	6.5200	5.8900	9.6

confirmative tests. Table 8 shows the confirmative test results obtained through both the approaches along with the optimal parametric setting with obtained value of overall utility index.

The calculated values of the overall utility index for the confirmatory test are found to be 6.21 and 5.89 with errors value of 10.1% and 9.6% for QPSO and PSO respectively. From the table, it can be clearly noticed that the results obtained through QPSO algorithm is more favorable to achieve improved machining efficiency.

7. Conclusions

Although Inconel 718 has wide-spread application, its machining both in conventional and non-conventional methods becomes difficult due to low thermal conductivity. In this work, an extensive experimental investigation has been carried out to analyse the effect of various electrode materials on the machinability of Inconel 718 super alloy in the EDM process. It is observed that material removal rate can be improved through the use of graphite tool but surface roughness and radial overcut are seriously affected due to high discharge energy. Brass can be used as tool electrode when better surface integrity is desired but the material removal rate is rather less. As far as tool wear is concerned, graphite tool performs superior to copper and brass tool. A hybrid approach of utility concept embedded with QPSO and PSO algorithms have been proposed and compared for obtaining best parametric setting for EDM process. From the performance comparison curve of both the algorithms, it is observed that QPSO provides better result than PSO owing to inherent capability of avoiding premature convergence. The optimal parametric setting obtained through both approaches is validated by conducting confirmative tests. The test results reveal that QPSO provides better solution in comparison to PSO resulting in improved machining efficiency. This analysis helps in identifying the important process parameters which can be effectively controlled to reduce the cost of machining, experimentation time and experimental error to increase productivity and quality of the process.

In spite of several major findings obtained through this study, analysis on recast layer formation, surface integrity and microstructure of the machined surface can be considered as some of the key limitations of the research. Numerical analysis can be carried out on this experimental investigation. In this work, QPSO has been applied without considering any constraints. In future, process related constraints can be incorporated during formulation of optimization problem.

References

- [1] H. Sidhom, F. Ghanem, T. Amadou, G. Gonzalez, C. Braham, Effect of electro discharge machining (EDM) on the AISI316L SS white layer microstructure and corrosion resistance, *Int. J. Adv. Manuf. Technol.* 65 (1–4) (2013) 141–153.
- [2] S. Assarzadeh, M. Ghoreishi, Statistical modeling and optimization of process parameters in electro-discharge machining of cobalt-bonded tungsten carbide composite (WC/6% Co), *Procedia CIRP* 6 (2013) 463–468.
- [3] S. Habib, A. Okada, S. Ichii, Effect of cutting direction on machining of carbon fibre reinforced plastic by electrical discharge machining process, *Int. J. Mach. Mach. Mater.* 13 (4) (2013) 414–427.
- [4] S.H. Lee, X.P. Li, Study of the effect of machining parameters on the machining characteristics in electrical discharge machining of tungsten carbide, *J. Mater. Process. Technol.* 115 (3) (2001) 344–358.
- [5] P. Kuppam, S. Narayanan, A. Rajadurai, Effect of process parameters on material removal rate and surface roughness in electric discharge drilling of Inconel 718 using graphite electrode, *Int. J. Manuf. Technol. Manage.* 23 (3–4) (2011) 214–233.
- [6] A. Majumder, P.K. Das, A. Majumder, M. Debnath, An approach to optimize the EDM process parameters using desirability-based multi-objective PSO, *Production and Manufacturing Research* 2 (1) (2014) 228–240.
- [7] U. Aich, S. Banerjee, Modeling of EDM responses by support vector machine regression with parameters selected by particle swarm optimization, *Appl. Math. Model.* 38 (11) (2014) 2800–2818.
- [8] C.P. Mohanty, S.S. Mahapatra, M.R. Singh, A particle swarm approach for multi-objective optimization of electrical discharge machining process, *J. Intell. Manuf.* (2014), <http://dx.doi.org/10.1007/s10845-014-0942-3>.
- [9] J. Kennedy, R. Eberhart, Particle swarm optimization, *Proceedings of IEEE International Conference on Neural Network Washington USA November/December 4* (1995) 1942–1948.
- [10] Y. Shi, R. Eberhart, A modified particle swarm optimizer, in: *Evolutionary Computation Proceedings, 1998. IEEE World Congress on Computational Intelligence*, 1998, pp. 69–73.
- [11] M.R. Singh, S.S. Mahapatra, A swarm optimization approach for flexible flow shop scheduling with multiprocessor tasks, *Int. J. Adv. Manuf. Technol.* 62 (1) (2012) 267–277.
- [12] H. Yoshida, K. Kawata, Y. Fukuyama, S. Takayama, Y. Nakanishi, A particle swarm optimization for reactive power and voltage control considering voltage security assessment, *IEEE Trans. Power Syst.* 15 (4) (2000) 1232–1239.
- [13] A.H. Ertas, Optimization of fiber-reinforced laminates for a maximum fatigue life by using the particle swarm optimization, Part I. *Mech. Compos. Mater.* 48 (6) (2013) 705–716.
- [14] A.H. Ertas, Optimization of fiber-reinforced laminates for a maximum fatigue life by using the particle swarm optimization, Part II. *Mech. Compos. Mater.* 49 (1) (2013) 107–116.
- [15] M.R. Singh, S.S. Mahapatra, R. Mishra, Robust scheduling for flexible job shop problems with random machine breakdowns using a quantum behaved particle swarm optimisation, *Int. J. Serv. Oper. Manage.* 20 (1) (2015) 1–20.
- [16] M. Xi, J. Sun, W. Xu, An improved quantum-behaved particle swarm optimization algorithm with weighted mean best position, *Appl. Math. Comput.* 205 (2) (2008) 751–759.
- [17] J. Sun, W. Xu, B. Feng, A global search strategy of quantum-behaved particle swarm optimization, in: *Cybernetics and Intelligent Systems, 2004 IEEE Conference on IEE*, (1), 2004, pp. 111–116.
- [18] J. Sun, W. Xu, B. Feng, Adaptive parameter control for quantum-behaved particle swarm optimization on individual level, 2005 IEEE International Conference on Systems, Man and Cybernetics, 4, 2005, pp. 3049–3054.
- [19] S. Prabhu, B.K. Vinayagam, Multi objective optimisation of SWCNT-based electrical discharge machining process using grey relational and fuzzy logic analysis, *Int. J. Mach. Mach. Mater.* 13 (4) (2013) 439–463.
- [20] S. Dewangan, C.K. Biswas, Optimisation of machining parameters using grey relation analysis for EDM with impulse flushing, *Int. J. Mechatronics Manuf. Syst.* 6 (2) (2013) 144–158.
- [21] V.K. Meena, M.S. Azad, S. Mitra, Effect of flushing condition on deep hole micro-EDM drilling, *Int. J. Mach. Mach. Mater.* 12 (4) (2012) 308–320.
- [22] N. Beri, A. Kumar, S. Maheshwari, C. Sharma, Optimisation of electrical discharge machining process with CuW powder metallurgy electrode using grey relation theory, *Int. J. Mach. Mach. Mater.* 9 (1–2) (2011) 103–115.
- [23] V. Senthilkumar, M. Chandrasekar Reddy, Performance analysis of Cu-B4C metal matrix composite as an EDM electrode, *Int. J. Mach. Mach. Mater.* 11 (1) (2012) 36–50.
- [24] J. Wang, F. Han, Simulation model of debris and bubble movement in consecutive-pulse discharge of electrical discharge machining, *Int. J. Mach. Tools Manuf* 77 (2014) 56–65.
- [25] Y. Shen, Y. Liu, Y. Zhang, B. Tan, R. Ji, B. Cai, C. Zheng, Determining the energy distribution during electric discharge machining of Ti-6Al-4V, *Int. J. Adv. Manuf. Technol.* 70 (1–4) (2014) 11–17.
- [26] S. Tripathy, D.K. Tripathy, Multi-attribute optimization of machining process parameters in powder mixed electro-discharge machining using TOPSIS and grey relational analysis, *Eng. Sci. Technol., Int. J.* (2015).
- [27] G. Talla, D.K. Sahoo, S. Gangopadhyay, C.K. Biswas, Modeling and multi-objective optimization of powder mixed electric discharge machining process of aluminum/alumina metal matrix composite, *Eng. Sci. Technol., Int. J.* 18 (3) (2015) 369–373.

- [28] G. Talla, S. Gangopadhyay, C.K. Biswas, Multi response optimization of powder mixed electric discharge machining of aluminum/alumina metal matrix composite using grey relation analysis, *Proc. Mater. Sci.* 5 (2014) 1633–1639.
- [29] B.B. Nayak, S.S. Mahapatra, Optimization of WEDM process parameters using deep cryo-treated Inconel 718 as work material, *Eng. Sci. Technol., Int. J.* (2015).
- [30] J.M. Jafferson, P. Hariharan, Machining performance of cryogenically treated electrodes in microelectric discharge machining: A comparative experimental study, *Mater. Manuf. Processes* 28 (4) (2013) 397–402.
- [31] S.S. Gill, J. Singh, Effect of deep cryogenic treatment on machinability of titanium alloy (Ti-6246) in electric discharge drilling, *Mater. Manuf. Processes* 25 (6) (2010) 378–385.
- [32] J. Kapoor, S. Singh, J.S. Khamba, Effect of cryogenic treated brass wire electrode on material removal rate in wire electrical discharge machining, *J. Mech. Eng. Sci.* (2012). 0954406212438804.
- [33] S.S. Paramashivan, J. Mathew, S. Mahadevan, Mathematical modeling of aerosol emission from die sinking electrical discharge machining process, *Appl. Math. Model.* 36 (4) (2012) 1493–1503.
- [34] S.N. Joshi, S.S. Pande, Development of an intelligent process model for EDM, *Int. J. Adv. Manuf. Technol.* 45 (3–4) (2009) 300–317.
- [35] S.N. Joshi, S.S. Pande, Thermo-physical modeling of die-sinking EDM process, *J. Manuf. Processes* 12 (1) (2010) 45–56.
- [36] C.P. Mohanty, J. Sahu, S.S. Mahapatra, Thermal-structural analysis of electrical discharge machining process, *Proc. Eng.* 51 (2013) 508–513.
- [37] Y. Chen, S.M. Mahdivian, Analysis of electro-discharge machining process and its comparison with experiments, *J. Mater. Process. Technol.* 104 (1) (2000) 150–157.
- [38] J. Nayak, B. Naik, H.S. Behera, A novel nature inspired firefly algorithm with higher order neural network: performance analysis, *Eng. Sci. Technol., Int. J.* (2015).
- [39] M. Balasubramanian, Prediction of optimum weld pool geometry of PCTIG welded titanium alloy using statistical design, *Eng. Sci. Technol., Int. J.* (2015).
- [40] M.P. Satpathy, B.R. Moharana, S. Dewangan, S.K. Sahoo, Modeling and optimization of ultrasonic metal welding on dissimilar sheets using fuzzy based genetic algorithm approach, *Eng. Sci. Technol., Int. J.* 18 (4) (2015) 634–647.
- [41] P. Cavaliere, A. Perrone, A. Silvello, Multi-objective optimization of steel nitriding, *Eng. Sci. Technol., Int. J.* (2015).
- [42] S. Padhee, N. Nayak, S.K. Panda, P.R. Dhal, S.S. Mahapatra, Multi-objective parametric optimization of powder mixed electro-discharge machining using response surface methodology and non-dominated sorting genetic algorithm, *Sadhana* 37 (2) (2012) 223–240.
- [43] M.K. Pradhan, C.K. Biswas, Neuro-fuzzy and neural network-based prediction of various responses in electrical discharge machining of AISI D2 steel, *Int. J. Adv. Manuf. Technol.* 50 (5–8) (2010) 591–610.
- [44] M.K. Pradhan, R. Das, Recurrent neural network estimation of material removal rate in electrical discharge machining of AISI D2 tool steel, *Proc. Inst. Mech. Eng., Part B: J. Eng. Manuf.* 225 (3) (2011) 414–421.
- [45] S.H. Yang, J. Srinivas, S. Mohan, D.M. Lee, S. Balaji, Optimization of electric discharge machining using simulated annealing, *J. Mater. Process. Technol.* 209 (9) (2009) 4471–4475.
- [46] R.S. Walia, H.S. Shan, P. Kumar, Multi-response optimization of CFAAFM process through Taguchi method and utility concept, *Mater. Manuf. Processes* 21 (8) (2006) 907–914.
- [47] B.C. Routara, S.D. Mohanty, S. Datta, A. Bandyopadhyay, S.S. Mahapatra, Optimization in CNC end milling of UNS C34000 medium leaded brass with multiple surface roughness characteristics, *Sadhana* 35 (5) (2010) 619–629.
- [48] H. Modares, A. Alfi, M.B.N. Sistani, Parameter estimation of bilinear systems based on an adaptive particle swarm optimization, *Eng. Appl. Artif. Intell.* 23 (7) (2010) 1105–1111.
- [49] M. Clerc, J. Kennedy, The particle swarm-explosion, stability, and convergence in a multidimensional complex space, *IEEE Trans. Evol. Comput.* 6 (1) (2002) 58–73.